

## FE simulation of S-N curves for a riveted connection using two-stage fatigue models

José A.F.O. Correia<sup>\*1</sup>, Abílio M.P. de Jesus<sup>1</sup>, António L.L. Silva<sup>1</sup>, Bruno Pedrosa<sup>2</sup>, Carlos Rebelo<sup>2</sup> and Rui A.B. Calçada<sup>1</sup>

<sup>1</sup>Faculty of Engineering, University of Porto, Rua Dr. Roberto Frias, 4200-465 Porto, Portugal

<sup>2</sup>Department of Civil Engineering, University of Coimbra, Rua Luis Reis Santos, 3030-788 Coimbra, Portugal

(Received December 30, 2016, Revised July 4, 2017, Accepted October 27, 2017)

**Abstract.** Inspections of ancient metallic bridges have illustrated fatigue cracking in riveted connections. This paper presents a comparison between two alternative finite element (FE) models proposed to predict the fatigue strength of a single shear and single rivet connection. The first model is based on solid finite elements as well as on contact elements, to simulate contact between the components of the connection. The second model is built using shell finite elements in order to model the plates of the riveted connection. Fatigue life predictions are carried out for the shear splice, integrating both crack initiation and crack propagation lives, resulting from the two alternative FE models. Global fatigue results, taking into account several clamping stresses on rivet, are compared with available experimental results. Proposed comparisons between predictions and experimental data illustrated that the proposed two-stage model yields consistent results.

**Keywords:** fatigue; S-N curve; finite element model; riveted connections; ancient bridges

---

### 1. Introduction

In the late XIX and early XX century many riveted steel bridges were built in Europe and North America and for economic reasons most of them are still in service despite the accumulated fatigue damage may jeopardize the bridge operation (Blasón *et al.* 2016). Moreover, an increasing in the traffic intensity, both in railway and highway bridges, has been verified which makes the safety a major concern for authorities. The fatigue assessment of these bridges is not a straightforward task due to the high uncertainties associated with the applied loading and fatigue phenomenon in general (Lesiuk *et al.* 2015). The maintenance and safety of existing bridges is a major concern of governmental agencies. In order to assure high safety levels in old riveted steel bridges, governmental agencies have to fund maintenance and retrofitting projects. Those projects demand residual life calculations of existing bridges in operation taking into account fatigue as a progressive damaging mechanism (Kwad *et al.* 2017, Liu *et al.* 2017). A consistent residual life prediction should be based on actual fatigue data from bridge members to assess (Lalthlamuana *et*

---

\*Corresponding author, Ph.D., E-mail: [jacorreia@inegi.up.pt](mailto:jacorreia@inegi.up.pt)

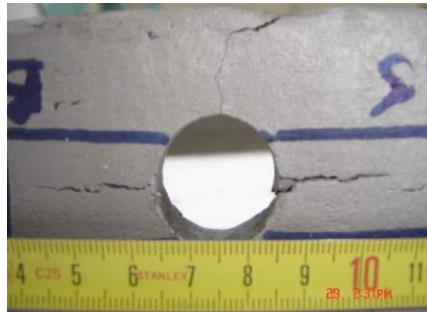


Fig. 1 Example of fatigue cracks emanating from rivet hole (Natal Jorge *et al.* 2006)

*al.* 2013).

Fatigue issues are not an exclusive concern of old riveted bridges. Fatigue analyses are also carried out on offshore wind turbine structures and finite element models (FEM) of connections are adopted to perform local fatigue analyzes. Those analyses are useful to estimate the contribution of the fatigue initiation phase (Alati *et al.* 2014, Jovašević *et al.* 2016, Öztürk *et al.* 2016). Numerical analyses are also used to evaluate the fatigue behavior of connections considering 3D finite elements (Habashizadeh Asl *et al.* 2013), and allows parametric studies on material properties and geometric features of connections (Lim *et al.* 2013). As an alternative to classic finite element method, numerical techniques based on the generalized finite element method and the partition of unit method, which is called of extended finite element method (XFEM) are also often applied. The XFEM method is used by Nanda (Nanda *et al.* 2016) to make the fatigue and fracture analysis of cracked stiffened panels.

This paper proposes a fatigue analysis of a single shear riveted connection by means of the finite element method. In particular, a comparison between two types of finite element models is performed with the particular aim of predicting the fatigue strength of a riveted connection. The estimates of the total fatigue life resulting from the application of the two models are compared between each other and with available experimental results. The fatigue life is simulated using a procedure that accounts independently for the fatigue crack initiation and propagation phases.

The fatigue crack initiation is predicted through the local strain approaches based on Basquin (Basquin 1910), Coffin (Coffin 1954) and Manson (Manson 1954) relations. Since these approaches require the elastoplastic strains at the critical locations, empiric elastoplastic analyses are performed using the mathematical representation of the cyclic stress-strain curve of the material proposed by Ramberg and Osgood (Ramberg and Osgood 1943), together with the Neuber (Neuber 1961) analysis for notched components.

In order to complement the model, Linear Elastic Fracture Mechanics (LEFM) analyses were undertaken to assess the number of cycles to propagate the crack until failure. A constant depth crack emanating from the rivet hole and propagating perpendicularly to main principal stress was modelled. This type of crack is usual in riveted joints as illustrated in Fig. 1. Stress intensity factors were evaluated using the Virtual Crack Closure Technique (Krueger 2002) which was applied to process results of FE cracked models. The stress intensity factors were used to integrate the Paris's law (Paris and Erdogan 1963) of the material to reach the propagation cycles.

Based on the prediction model (initiation and propagation) S-N curves for a riveted connection, taking into account several clamping effects on rivet are presented. The beneficial effect of clamping effect of rivets on the fatigue behavior of riveted connections (Correia *et al.* 2011, De

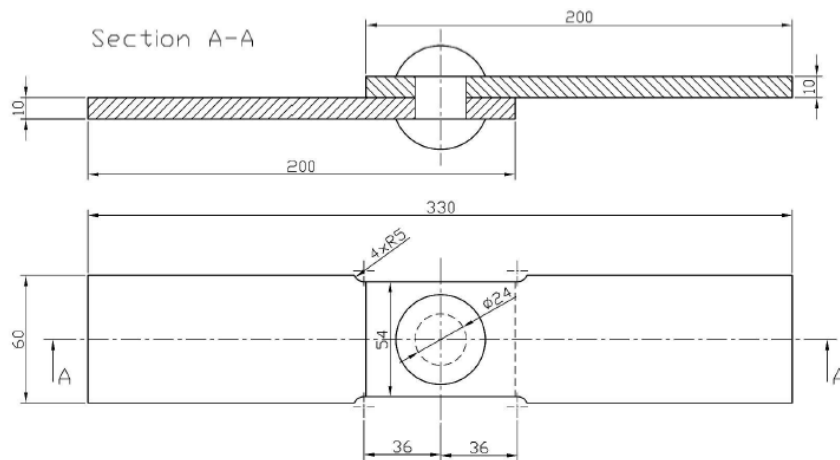


Fig. 2 Geometry of the single shear and single rivet joint (dimensions in mm)

Jesus *et al.* 2014, Sanches *et al.* 2015) is demonstrated.

The fatigue life is predicted for a riveted joint with a single shear plane and with a single rivet, which was cut from an original bracing member extracted from the Portuguese riveted Trezói railway bridge (see Fig. 2). The specification of the fatigue tests performed for this connection are published elsewhere (Silva 2006, Correia 2008, Correia *et al.* 2008, 2009, Correia *et al.* 2010, De Jesus *et al.* 2010, 2011, 2015). A series of specimens was prepared and fatigue tests under stress  $R$ -ratio equal to 0.1 were performed. The main failure mode corresponded to the initiation of fatigue cracks in the rivet hole that propagated in the resistant section (plane containing the axis of the rivet and is normal to the direction of the load). Resulting experimental results are compared with the global prediction of the  $S$ - $N$  curve obtained based on two types of finite element models proposed (solid model and shell model). The use of shell elements can be understood as a computational alternative to the solid elements that may lead to lower computational costs, and therefore could be an option for the simulation of complex riveted joints of real bridges, which may present a significant number of rivets.

## 2. Fatigue modelling of a single shear riveted connection

### 2.1 Fatigue crack initiation modelling

Crack initiation has been addressed by local approaches. These approaches usually use the local elastoplastic strains and/or stresses to formulate a fatigue damage parameter that is directly correlated with the number of cycles or reversals to failure. The Morrow (1965) relation is a very well-known relation that relates the total elastoplastic strain with the number of reversals to failure

$$\frac{\Delta\varepsilon}{2} = \frac{\sigma'_f}{E} (2N_f)^b + \varepsilon'_f (2N_f)^c \quad (1)$$

where:  $\Delta\varepsilon$  is the total elastoplastic strain range;  $\sigma'_f$  is the fatigue strength coefficient;  $b$  is the fatigue strength exponent;  $\varepsilon'_f$  is the fatigue ductility coefficient;  $c$  is the fatigue ductility exponent;

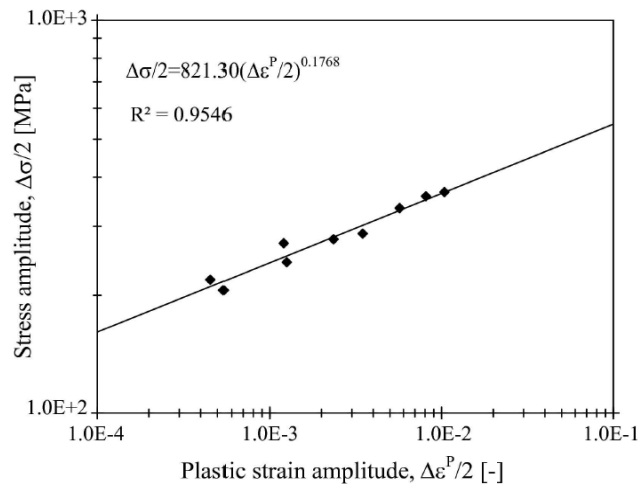


Fig. 3 Cyclic elastoplastic properties of the material from the Trezói bridge

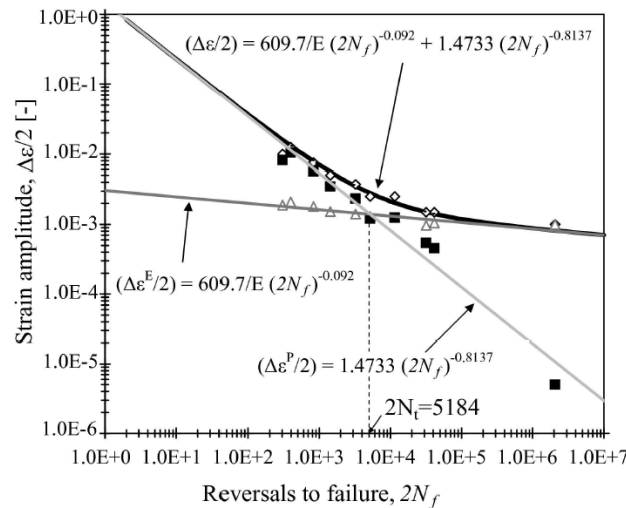


Fig. 4 Strain-life data of the material from the Trezói bridge

$E$  is the Young modulus and  $2N_f$  is the number of reversals to failure. The Morrow relation resulted from the superposition of the Coffin-Manson (Coffin and Manson 1954) and Basquin (Basquin 1910) relations. While the Coffin-Manson relation correlates the plastic strain amplitude with the number of reversals, the Basquin relation correlates the elastic strain amplitude with the number of reversals. It is generally accepted that strain-life relation as proposed by Morrow is used to assess the number of cycles to initiate a macroscopic crack.

In order to evaluate the total elastoplastic strains at the critical locations, cyclic elastoplastic FE analysis can be performed or simplified formulae for elastoplastic analysis applied. Often, simplified formulae consist in the application of Neuber (Neuber 1961) analysis applied in conjunction with a mathematical description of the material uniaxial cyclic elastoplastic curve, such as the Ramberg-Osgood (Ramberg and Osgood 1943) relation, resulting the following system of equations, valid for cyclic loading

$$\frac{\Delta\sigma^2}{E} + 2 \cdot \Delta\sigma \left( \frac{\Delta\sigma}{2K'} \right)^{1/n'} = \frac{K_t^2 \cdot \Delta\sigma_{nom}^2}{E} \quad (2)$$

$$\Delta\varepsilon = \frac{\Delta\sigma}{E} + 2 \cdot \left( \frac{\Delta\sigma}{2K'} \right)^{1/n'}$$

where:  $K'$  and  $n'$  are respectively the cyclic strength coefficient and the strain hardening exponent,  $K_t$  is the elastic stress concentration factor,  $\Delta\sigma_{nom}$  is the nominal stress range,  $\Delta\sigma$  and  $\Delta\varepsilon$  are the local stress and strain ranges.

The material properties needed to implement the fatigue crack initiation model (Eqs. (1) and (2)) were determined experimentally for the original material from the riveted connection and are published elsewhere (Correia 2008, Correia *et al.* 2008, De Jesus *et al.* 2008, 2011, 2015). Figs. 3 and 4 summarize the cyclic and strain-life properties of the material from the Trezói bridge.

## 2.2 Fatigue crack propagation modelling

The fatigue crack propagation modelling was performed in the context of Linear Elastic Fracture Mechanics (LEFM). As soon as the crack is initiated, a propagation model is required to evaluate the number of cycles to achieve the connection failure. The number of cycles to propagate a crack can be determined, integrating a propagation law, such as the one proposed by Paris (Paris and Erdogan 1963)

$$da/dN = C(\Delta K)^m \quad (3)$$

where:  $C$  and  $m$  are material constants,  $\Delta K$  is the stress intensity factor range and  $da/dN$  is the crack growth rate.

The constants of the Paris law were obtained experimentally for the material extracted from the Trezói bridge (Correia 2008, Correia *et al.* 2008, De Jesus *et al.* 2008, 2011, 2015):  $C=1.1054 \times 10^{-16}$  and  $m=4.0944$ , for  $R=0.0$  ( $da/dN$  in mm/cycle with  $\Delta K$  in  $\text{N}\cdot\text{mm}^{-1.5}$ , see Fig. 5).

In this paper we analyse a crack emanating from the rivet hole, as illustrated in Fig. 6: a through thickness crack of uniform depth,  $a$ , was simulated. An important assumption of a crack initiated on both sides of the rivet hole in one side plate, is taken. This assumption is used in the crack propagation modelling. Also, for the sake of simplicity it is assumed that the crack propagates the same amount on both sides of the hole and remains always a constant depth crack. Thus, the number of cycles to propagate de crack can be derived as

$$N_f = \frac{1}{C} \int_{a_i}^{a_f} \frac{1}{\Delta K^m} da \quad (4)$$

To perform the previous integration, the stress intensity range must be expressed as a function of the crack length,  $a$ . The integral can be approximately evaluated assuming successive crack increments,  $\Delta a$ , with constant stress intensity factor range, yielding an increment in the number of cycles to failure

$$\Delta N = \frac{1}{C} \frac{1}{\Delta K^m} \Delta a \quad (5)$$

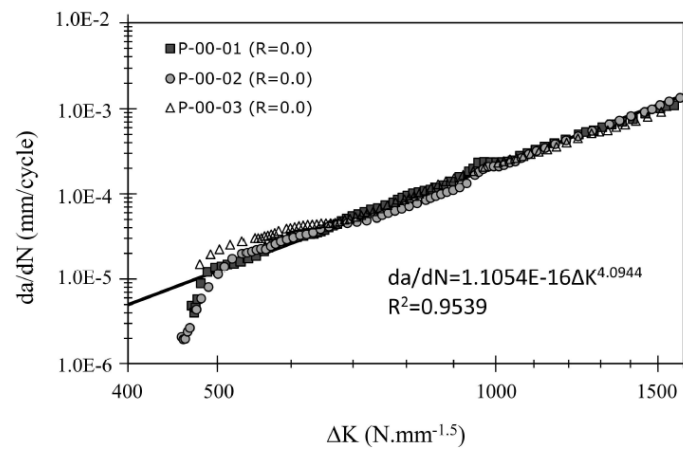


Fig. 5 Fatigue crack propagation data of the material from the Trezói bridge, for  $R=0.0$

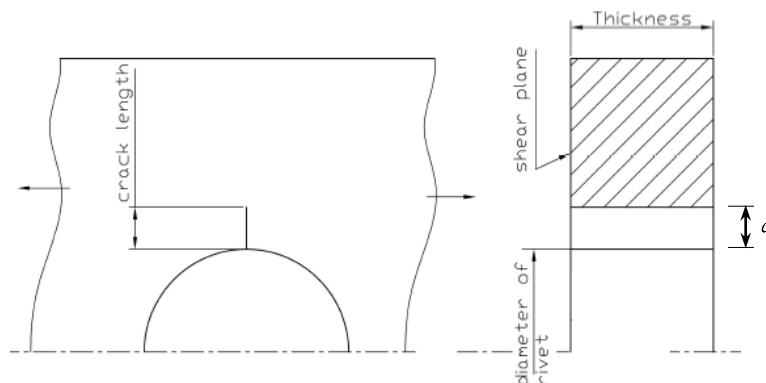


Fig. 6 Through thickness crack configuration

The previous approximation leads to the exact integral as the crack increment approaches to zero. In the evaluation of the propagation period, the crack is propagated until the maximum stress intensity approaches the material toughness, i.e., the maximum stress intensity factor registered during the crack propagation tests for stress  $R$ -ratio equal to 0.0:  $\Delta K \approx 1600 \text{ N} \cdot \text{mm}^{-1.5}$  (see Fig. 5).

### 3. FE MODELS OF THE RIVETED CONNECTION

#### 3.1 Models for stress concentration factor computation for the uncracked joint

In order to simulate the crack initiation phase of the riveted connection in study, we propose two finite element models without cracks. In one model, the plates of connection were modelled with solid elements; in the other model, the plates of the connection were modelled with shell elements. In both models, the rivet was modelled with solid elements. The models were built using ANSYS® code (SAS 2008).

Models were built taking into account only half of the connection, taking advantage of the symmetry plane. The models were built in agreement with the dimensions of Fig. 2. The nodes of

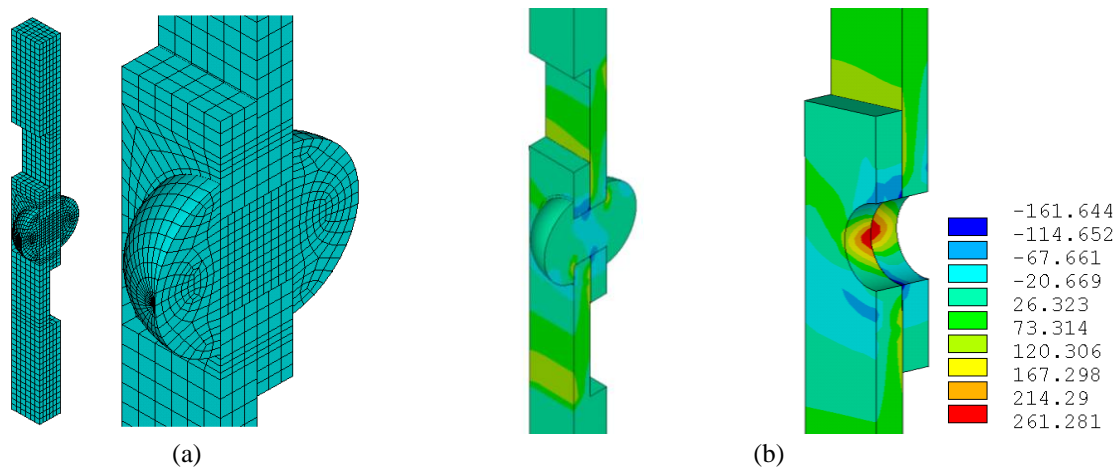


Fig. 7 Solid finite element model of the rivet joint: (a) mesh of the model without cracks; (b)  $\sigma_y$  stress field in loading direction in MPa (imposed remote displacement of 0.1 mm)

the symmetry plane were restricted in the direction perpendicular to the symmetry plane; top nodes of the connection were restricted in the two directions within the plane normal to the loading and a displacement  $d_{max}=0.1$  mm, was applied in the loading direction; the nodes of the bottom of the model were restricted in all directions. Both steel plates and rivets were modelled as isotropic and elastic materials ( $E=210$  GPa,  $\nu=0.27$ ). Proposed models are only capable of simulating the elastic behaviour of the joint. Nevertheless, the finite element model is non-linear due to the contact problem. Therefore, an incremental analysis was used. Both surfaces in contact were assumed flexible. These models are used to evaluate the of elastic stress concentration factor. Loading is applied incrementally: 10 increments equal of 0.01 mm (De Jesus and Correia 2008, De Jesus *et al.* 2010, 2011, 2014, Correia *et al.* 2011, Sanches *et al.* 2015).

The simulations were performed using the Augmented Lagrange contact algorithm along with the Coulomb friction model, taking into account three different friction coefficients:  $\mu=0$ ,  $\mu=0.3$  and  $\mu=0.6$ .

The Augmented Lagrange algorithm requires the definition of normal penalty stiffness factor (FKN). Present simulations covered FKN values equal to 0.01, 0.1 and 1.0. Another relevant contact parameter to be used in conjunction with the Augmented Lagrange method is FTOLN. FTOLN values equal to 0.01, 0.05 and 0.1 were simulated. For all other contact parameters not mentioned here, default values were adopted (SAS 2008).

Simulations were carried out considering a null gap. Also, it was imposed clamping effects on rivets by applying a  $\Delta T$  to rivet and associating to the rivet orthotropic thermal expansion properties, including a coefficient of thermal expansion,  $\alpha_z$ , equal to  $10^{-5}/^\circ\text{C}$  (in the direction of the axis of rivet), and a final temperature,  $T_{final}$ , equal to  $25^\circ\text{C}$ . The clamping force on rivet was imposed by variation of the reference temperature,  $T_{ref}(T_{ref} \geq T_{final})$ . The properties of thermal expansion, in the transverse plane of the rivet, were considered null.

The elastic stress concentration factor,  $K_t$ , was evaluated dividing the maximum stress,  $\sigma_{y,max}$ , by the resistant area of the side plates, as follows

$$K_t = \left[ \sigma_{y,max} (W - d) t \right] / F \quad (6)$$

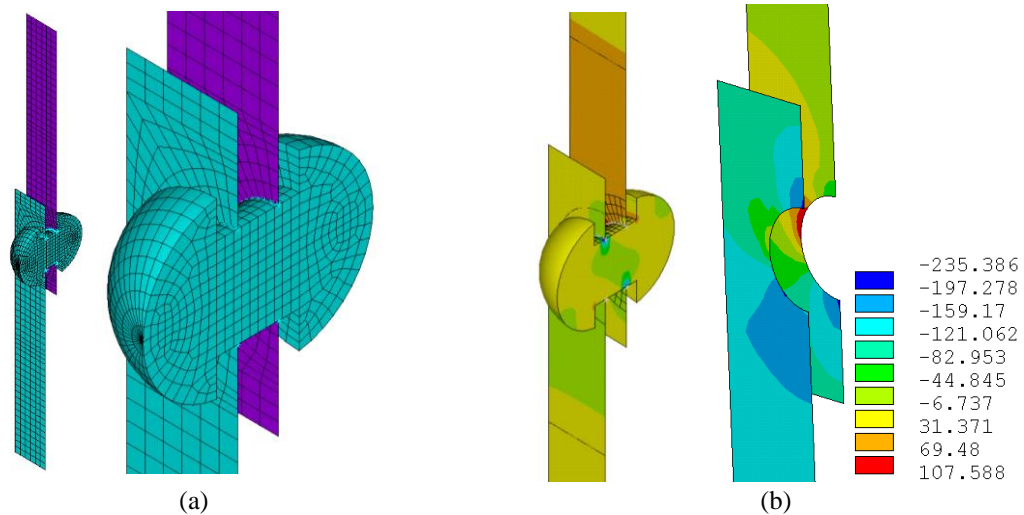


Fig. 8 Shell finite element model of the rivet joint: (a) mesh of the model without cracks; (b)  $\sigma_y$  stress field in the loading direction in MPa

where:  $W$  is the connection width,  $d$  is the rivet diameter,  $t$  is the plate thickness,  $F$  is the applied load and  $\sigma_{y,max}$  is the maximum stress according the loading direction, observed around the rivet dowel.

### 3.1.1 Solid finite element model

The riveted connection was modelled using solid iso-parametric twenty-noded finite elements (SOLID95). The contact between these plates and rivets was modelled with contact elements CONTA174 and TARGE170. Flexible contact pairs were considered (De Jesus and Correia 2008, De Jesus *et al.* 2010, 2011, 2014, Correia *et al.* 2011, Sanches *et al.* 2015). Fig. 7 illustrates the finite element mesh of the joint and the computed direct stress field along the loading direction. It appears that the extreme values of the stresses are observed in the holes and the stress distribution along the thickness is not uniform, being maxima near the shear plane. The stress field presented in the figure was derived for friction coefficient  $\mu=0.3$ , and contact parameters FKN=1.0 and FTOLN=0.01 or 0.1.

### 3.1.2 Shell finite element model

An alternative finite element model was constructed using shell elements for the plates. SOLID95 elements were used to model the rivet and shell elements (SHELL63) were used to model the plates of the connection. CONTA174, CONTA175 and TARGE170 elements were used to model the contact between the various elements of the connection (De Jesus *et al.* 2014, Sanches *et al.* 2015). Fig. 8 illustrates the corresponding finite element mesh of the joint and the resulting direct stress field along the loading direction. This figure presents the stress field for  $\mu=0.3$ , FKN=1.0 and FTOLN=0.01/0.1.

### 3.1.3 Stress concentration results

Figs. 9 and 10 illustrate the stress concentration factor,  $K_t$  for the solid and shell finite element models, respectively, take into account rivet clamping effects, friction coefficients, FKN and

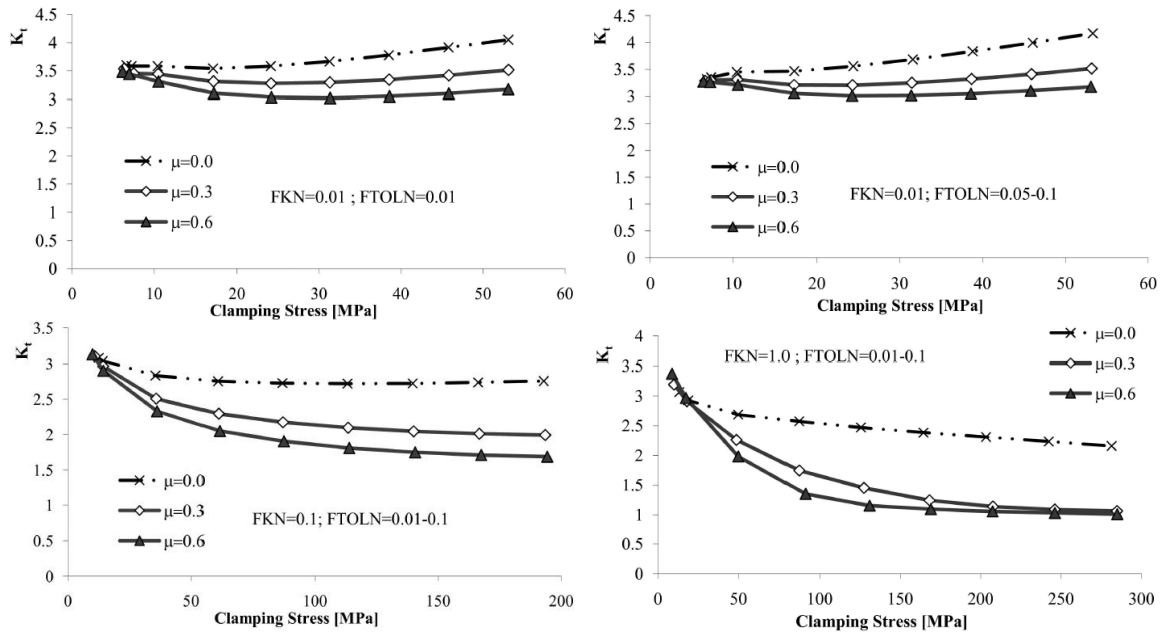


Fig. 9 Stress concentration factor evolution obtained with solid finite element model

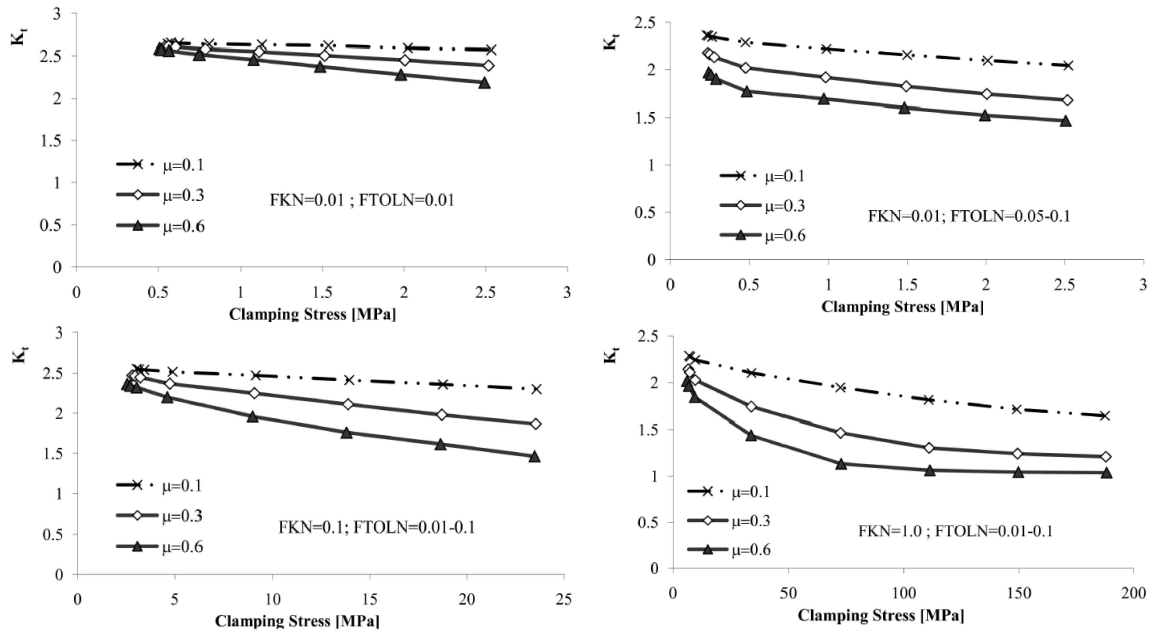


Fig. 10 Stress concentration factor evolution obtained with shell/solid finite element model

FTOLN. FKN equal to 0.01 produces physically inconsistent results, because  $K_t$  should decrease monotonically with the increase of the clamping stress and friction coefficient. The  $K_t$  must tend to unity with increasing clamping stress. So FKN=1.0 leads to consistent results, for the values of FTOLN in the range 0.01-0.1. Consequently, we will use in the prediction of fatigue strength,

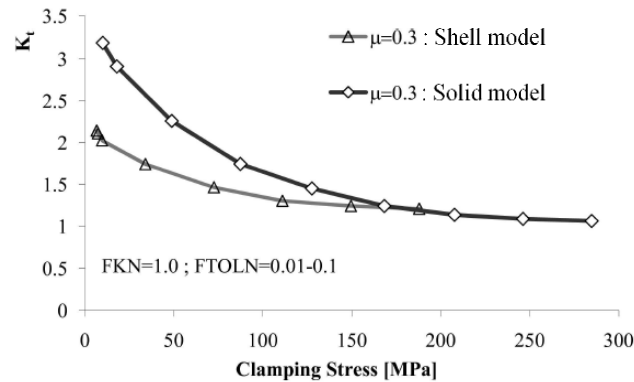


Fig. 11 Comparison of the stress concentration factors as a function of the clamping stresses resulting from the shell and solids finite elements models

contact parameters  $FKN=1.0$  and  $FTOLN=0.1$  (De Jesus *et al.* 2010, 2011, 2014, Correia *et al.* 2011). A friction coefficient  $\mu=0.3$  will be also adopted, which is a plausible value for the steel-steel contact and consistent with literature concerning riveted joints modelling (Imam and Righiniotis 2007).

Fig. 11 compares the results of  $K_t$  obtained with solid and shell FE models for various clamping stresses. The analysis of the graph shows a  $K_t$  tending to the unity. For values of clamping stresses lower than 150 MPa, it appears that the values of  $K_t$  are higher for the model with solid elements. The numerical values of  $K_t$  used in the crack initiation modelling were 2.35 and 3.28, respectively, for the model with shell elements and a model with solid elements. These values correspond to a value of clamping stress negligible, as is often considered for riveted joints.

### 3.2 Model for stress intensity factor computation of cracked joint

In order to simulate the fatigue crack propagation phase, finite element models of the connection with cracks emanating from the hole of a plate in a symmetrical configuration, taking into account the geometry of the Figs. 2 and 6, were executed. Fig. 12 illustrates the finite element meshes for the models with solid and shell elements, and their respective stress fields according the loading direction ( $y$ ) for various crack lengths, without rivet clamping effects. To simulate the crack propagation the following additional parameters were used:  $FKN=1.0$ ,  $FTOLN=0.1$  e  $\mu=0.3$  (De Jesus *et al.* 2010, 2014, Sanches *et al.* 2015).

The stress intensity factors were evaluated for both models using the modified virtual crack closure technique (Krueger 2002). Fig. 13 shows the evolution of the stress intensity factors normalized using the nominal stress defined by Eq. (5), for the solid and shell models. A consistent reduction of the stress intensity factors with the clamping stresses is observed. Figs. 14(a) and 14(b) compare the evolution of the stress intensity factors, as a function of crack length, for null and 34 MPa clamping stresses, respectively, which were evaluated using both finite element models. The analysis of the figure shows that the shell finite element model yields higher stress intensity results than the solid finite element model. This observation is contrary to the results obtained for the elastic stress concentration factors, which means that the shell model, when compared with the solid model, will underestimate the fatigue crack initiation phase and will overestimate the crack propagation phase.

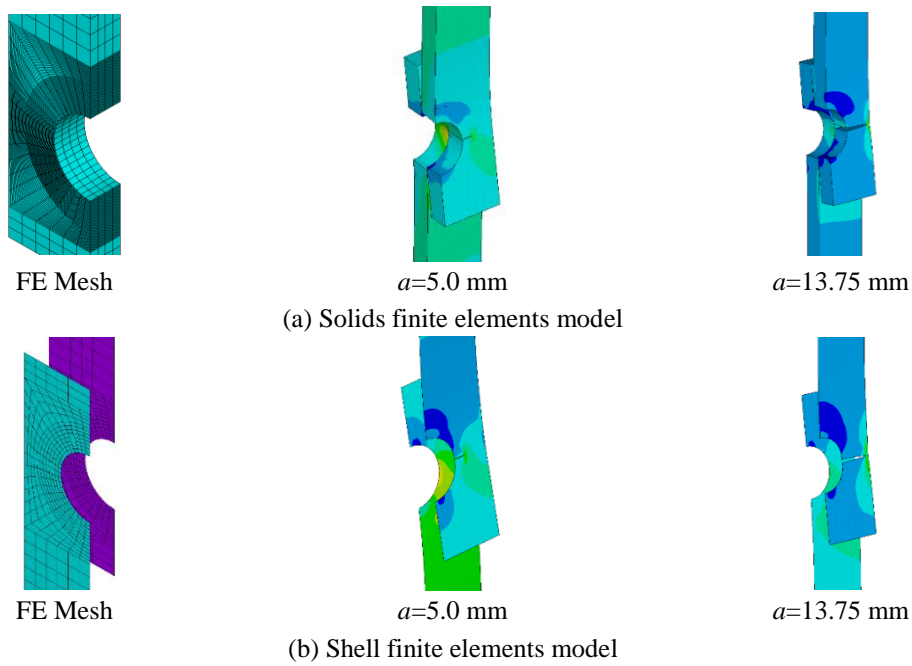


Fig. 12 Typical finite element meshes and  $\sigma_y$  stress field for several crack lengths ( $\Delta T=0^\circ\text{C}$ )

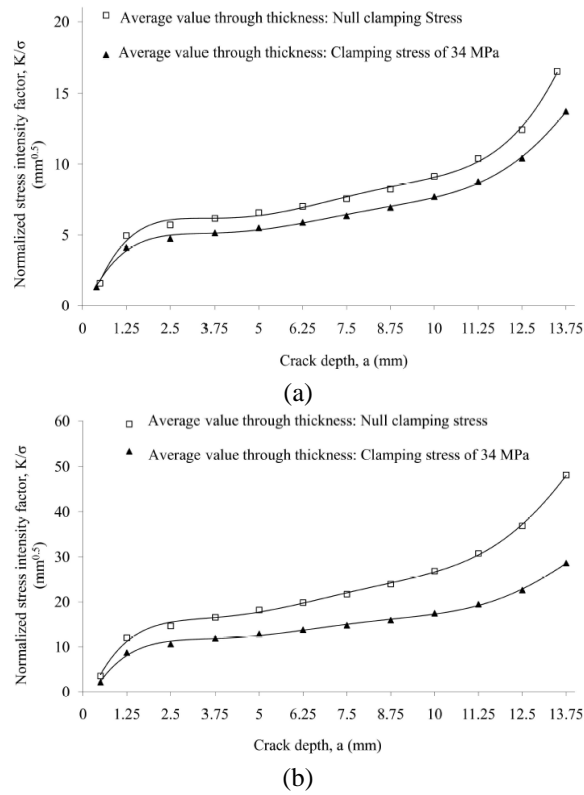


Fig. 13 Evaluation of the stress intensity factors with the crack length: (a) solid model and (b) shell model

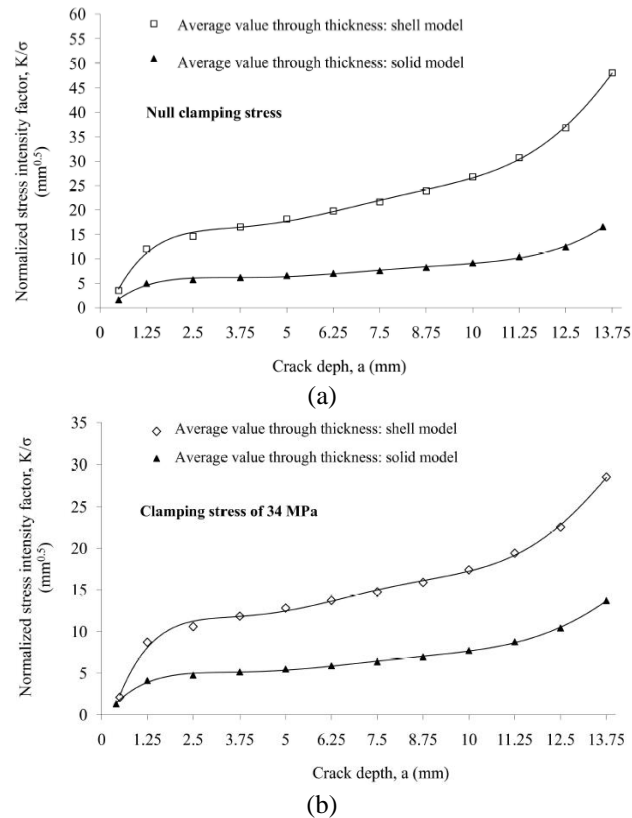


Fig. 14 Comparison of stress intensity factors obtained with solid and shell models: (a) null clamping and (b) clamping stress of 34 MPa

#### 4. Application and discussion

Figs. 15 and 16 show the fatigue strength predictions for the riveted connection under study, using the two proposed finite element models. In particular, the figures present the results of the crack initiation and propagation phases as well as the total fatigue life. For the same stress range level in both fatigue cracks initiation and propagation phases, the sum of the number of cycles to failure is made. The estimates took into account the influence of clamping stress effects. It was also considered an initiation criterion based on a crack length  $a_i=0.6$  mm.

From the analysis of the Figs. 15 and 16 it appears that the initiation phase is dominant in the model with shell elements, approaching satisfactorily to the global predictions. The propagation phase for the shell model shows relatively low values of fatigue lives, so it has negligible influence in the prediction of the global fatigue life for that model. The global predictions of the  $S-N$  curve for the shell model practically coincide with the experimental  $S-N$  curve.

The propagation curves for the model with solid elements have a slope higher than the experimental  $S-N$  curve. Again, the initiation curve for the solid model shows a slope very close to the experimental  $S-N$  curve, which is a symptom of the crack initiation dominated problem. It is also verified that the propagation phase is dominant for low-cycle fatigue regimes when the solid model is applied. In the same way as observed with the shell model, the crack initiation phase is

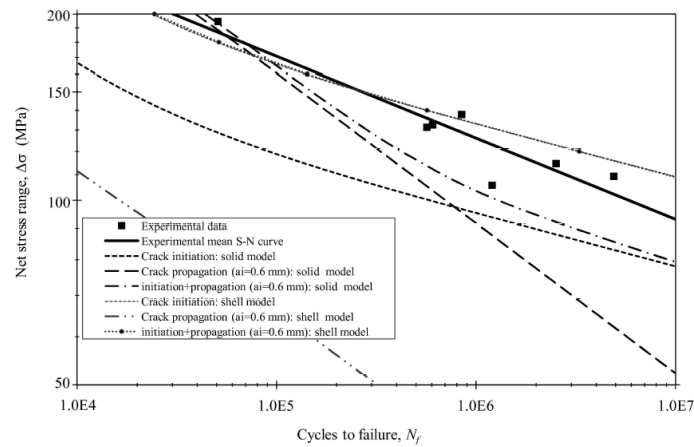


Fig. 15 Fatigue life predictions for the riveted connection for two proposed models: FKN=1.0; FTOLN=0.1;  $\mu=0.3$  and null clamping effects

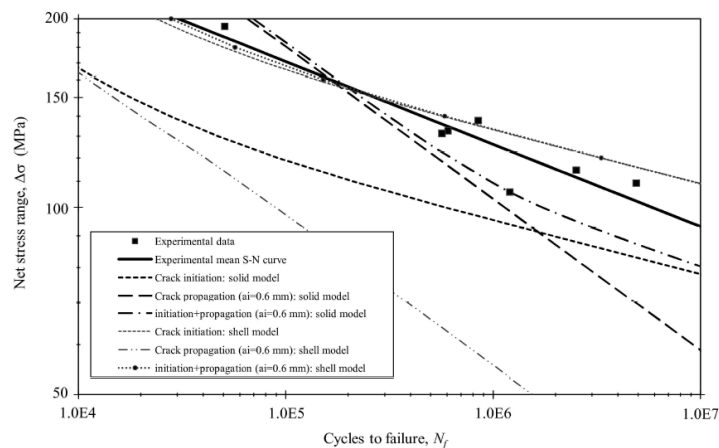


Fig. 16 Fatigue life predictions for the riveted connection for two proposed models: FKN=1.0; FTOLN=0.1;  $\mu=0.3$  and clamping stress of 34 MPa

dominant for high-cycle fatigue. The global S-N curves, simulated for the absence of clamping effects, show a very satisfactory approximation to the experimental S-N curve and it is clear that the only possibility to obtain S-N curves closer to the experimental curves is accounting for the crack initiation phase.

The fatigue crack initiation phase is dominant in both finite element analyses taking into account the contribution for the global S-N curve, when compared with the fatigue crack propagation phase. Furthermore, the fatigue crack propagation phase for low-cycle fatigue regimes is significant when compared with fatigue crack initiation phase.

The global S-N curve predicted with clamping stress of 34 MPa is slightly shifted upward, being almost coinciding with the experimental results, demonstrating the beneficial effect of the rivet clamping. It is evident the beneficial effects of clamping effects of rivet in prolonging fatigue life or increasing the fatigue strength. This effect is fully potentiated when bolted joints are used in structures to accomplish the joints.

## 5. Conclusions

The main conclusions of the study are summarized as follows:

- The proposed finite elements models constructed with contact elements were able to properly account for the local effects of the rivet;
- The analysis of results regarding the stress concentration factor evolution with the clamping effect of the rivet for the two proposed models, shows that the normal contact stiffness parameter,  $FKN=1.0$ , leads to consistent results since there is a monotonic decrease of  $K_t$  with increasing clamping;
- The modified virtual crack closure technique revealed as an efficient technique in determining the stress intensity factors, since it can be applied as a post-processing of finite elements model results;
- The finite element models were applied to demonstrate the beneficial effects in the fatigue strength of the joint on the clamping stress induced by the rivet. The estimated global  $S-N$  curves supported by the two FE models, without clamping effects, showed a very satisfactory approximation to the experimental  $S-N$  curve. With the presence of a clamping of 34 MPa the prediction is also satisfactory, when compared with the experimental  $S-N$  curve. But higher values of clamping stresses would result in non-conservative predictions which makes plausible a relative low clamping stress in the tested riveted joint;
- The proposed models based on independent estimates of the crack initiation and propagation, showed predictions very consistent with the available experimental results. The criterion for crack initiation based on a 0.6mm crack depth has proved to be a reasonable assumption and that fits the normal range established in the literature. For the shell element model the crack initiation is dominant. For the solid model, the propagation phase is a dominant phase in the low to medium-cycle fatigue;
- The shell model led to lower stress concentration factors than the solid model, however the prior model resulting in higher stress intensity factor estimates. This effect changed the crack initiation and propagation phases predictions, but a balance is verified resulting total fatigue lives reasonably consistent between the two models. Therefore, the two models are alternatives, the shell model representing a computational more efficient model.

## Acknowledgments

The authors acknowledge the Portuguese Science Foundation (FCT) for the financial support through the post-doctoral grant SFRH/BPD/107825/2015. Authors gratefully acknowledge the funding of SciTech-Science and Technology for Competitive and Sustainable Industries, R&D project NORTE-01-0145-FEDER-000022 cofinanced by Programa Operacional Regional do Norte (“NORTE2020”), through Fundo Europeu de Desenvolvimento Regional (FEDER).

## References

- Alati, N., Nava, V., Failla, G., Arena, F. and Santini, A. (2014), “On the fatigue behavior of support structures for offshore wind turbines”, *Wind Struct.*, **18**(2), 117-134.
- Balsón, S., Correia, J.A.F.O., De Jesus, A.M.P., Fernandez-Canteli, A. and Calçada, R.A.B. (2016), “A

- probabilistic analysis of Miner's law for different loading conditions", *Struct. Eng. Mech.*, **60**(1), 71-90.
- Basquin, O.H. (1910), "The exponential law of endurance tests", *Proc. ASTM*, **10**(II), 625-630.
- Coffin, L.F. (1954), "A study of the effects of the cyclic thermal stresses on a ductile metal", *Translat. ASME*, **76**, 931-950.
- Correia, J.A.F.O. (2008), "Development fatigue life predictions models for the riveted connection", M.Sc. Dissertation, University of Trás-os-Montes and Alto Douro, Portugal.
- Correia, J.A.F.O., De Jesus, A.M.P., Figueiredo, M.A.V., Ribeiro, A.S. and Fernandes, A.A. (2009), "Overview of recent Portuguese research on fatigue behaviour of ancient Portuguese riveted steel bridges", *Revist. Mecân. Exper.*, **16**, 73-79.
- Correia, J.A.F.O., De Jesus, A.M.P., Figueiredo, M.A.V., Ribeiro, A.S. and Fernandes, A.A. (2008), "Variability analysis of fatigue crack growth rates of materials from ancient Portuguese steel bridges", *Proceedings of the Bridge Maintenance, Safety and Management*, Korea, July.
- Correia, J.A.F.O., De Jesus, A.M.P., Figueiredo, M.V., Ribeiro, A.S. and Fernandes, A.A. (2008), "Fatigue assessment of riveted railway bridge connections. part I: Experimental investigations", *Proceedings of the 7th International Conference on Steel Bridges*, Guimarães, Portugal.
- Correia, J.A.F.O., De Jesus, A.M. and Silva, A.L.L. (2011), "Simulação por elementos finitos de curvas S-N de ligações rebitadas", *Revist. Mecân. Exper.*, **19**, 9-18.
- Correia, J.A.F.O., De Jesus, A.M.P., Silva, A.L.L. and Silva, J.F.N. (2010), "A procedure to derive probabilistic fatigue strength data for riveted joints", *sBridge Maintenance, Safety and Management*, Pennsylvania, U.S.A., July.
- De Jesus, A.M.J. and Correia, J.A.F.O. (2008), "Fatigue assessment of riveted railway bridge connections. Part II: Numerical investigations", *Proceedings of the 7th International Conference on Steel Bridges*, Guimarães, Portugal.
- De Jesus, A.M.P., Correia J.A.F.O., Ribeiro, A.S., Figueiredo, M.V. and Fernandes, A.A. (2008), "Low-cycle and crack growth fatigue data of a steel from the trezóí railway riveted bridge", *Proceedings of the 11th Portuguese Conference on Fracture*, Caparica, Portugal.
- De Jesus, A.M.P. and Correia, J.A.F.O. (2010), "Stress intensity factors evaluation for riveted beams applying FEA with VCCT", *Proceedings of the Bridge Maintenance, Safety and Management*, Pennsylvania, U.S.A., July.
- De Jesus, A.M.P., Da Silva, A.L.L., Figueiredo, M.V., Correia, J.A.F.O., Ribeiro, A.S. and Fernandes, A.A. (2011), "Strain-life and crack propagation fatigue data from several Portuguese old metallic riveted bridges", *Eng. Fail. Analy.*, **18**(1), 148-163.
- De Jesus, A.M.P., Pinto, H., Fernández-Canteli, A., Castillo, H. and Correia, J.A.F.O. (2010), "Fatigue assessment of a riveted shear splice based on a probabilistic model", *J. Fatigue*, **32**, 453-462.
- De Jesus, A.M.P., Silva A.L.L. and Correia J.A.F.O. (2014), "Fatigue of riveted and bolted joints made of puddle iron-a numerical approach", *J. Constr. Steel Res.*, **102**, 164-177.
- De Jesus, A.M.P., Silva, A.L.L. and Correia, J.A.F.O. (2015), "Fatigue of riveted and bolted joints made of puddle iron-an experimental approach", *J. Constr. Steel Res.*, **104**, 81-90.
- Habashizadeh Asl, M.H., Chenaglou, M.R., Abedi, K. and Hassan Afshin, H. (2013), "3D finite element modelling of composite connection of RCS frame subjected to cyclic loading", *Steel Compos. Struct.*, **15**(3), 281-298.
- Imam, B., Righiniotis, T.D. and Chryssanthopoulos, M.K. (2007), "Numerical modelling of riveted railway bridge connections for fatigue evaluation", *Eng. Struct.*, **29**(11), 3071-3081.
- Jorge, R.N., Ribeiro, A.S., Jesus, A.M.P., Figueiredo, M., Tavares de Castro, P.M.S. and Fernandes, A.A. (2006), *Eiffel Bridge-Viana Do Castelo. Results Evaluation of Experimental Program*, IDMEC/FEUP, Faculty of Engineering, University of Porto.
- Jovašević, S., Correia, J.A.F.O., Pavlović, M., Rebelo, C., De Jesus, A.M.P., Veljković, M. and Simões Da Silva, L. (2016), "Global fatigue life modelling of steel half-pipes bolted connections", *Proc. Eng.*, **160**, 278-284.
- Krueger, R. (2002), *The Virtual Crack Closure Technique: History, Approach and Applications*, Technical Report, NASA/CR-2002-211628 ICASE Report N.º 2002-10, NASA Langley Research Center Hampton.

- Kwad, J., Alencar, G., Jesus, A., Correia, José A.F.O., Calçada, R., Brownjohn, J. and Prakash, K. (2017), "Fatigue assessment of an existing bascule steel motorway bridge by finite element modelling", *J. Phys.*, **843**, 012038.
- Lalthlamuana, R. and Talukdar, S. (2013), "Rating of steel bridges considering fatigue and corrosion", *Struct. Eng. Mech.*, **47**(5), 643-660.
- Lesiuk, G., Szata, M. and Bocian, M. (2015), "The mechanical properties and the microstructural degradation effect in an old low carbon steels after 100-years operating time", *Arch. Civil Mech. Eng.*, **15**(4), 786-797.
- Lim, C., Choi, W. and Sumner, E.A. (2013), "Parametric study using finite element simulation for low cycle fatigue behavior of end plate moment connection", *Steel Compos. Struct.*, **14**(1), 57-71.
- Liu, Z., Hebdon, M.H., Correia, J.A.F.O., Carvalho, H., Vilela, P., De Jesus, A.M.P. and Calçada, R. (2017), "Fatigue life evaluation of critical details of the hercílio luz suspension bridge", *Proc. Struct. Integr.*, In Press.
- Manson, S.S. (1954), *Behaviour of Materials under Conditions of Thermal Stress*, NACA TN-2933, National Advisory Committee for Aeronautics.
- Morrow, J.D. (1965), *Cyclic Plastic Strain Energy and Fatigue of Metals in Internal Friction, Damping and Cyclic Plasticity*, American Society for Testing and Materials, Philadelphia, U.S.A., 45-87.
- Nanda Kumar, M.R., Ramachandra Murthy, A., Gopinath, S., Nagesh, R. and Iyer, N.R. (2016), "XFEM for fatigue and fracture analysis of cracked stiffened panels", *Struct. Eng. Mech.*, **57**(1), 65-89.
- Neuber, H. (1961), "Theory of stress concentration for shear-strained prismatic bodies with arbitrary nonlinear stress-strain law", *J. Appl. Mech.*, **28**, 544-550.
- Öztürk, F., Correia, J.A.F.O., Rebelo, C., De Jesus, A.M.P. and Simões Da Silva, L. (2016), "Fatigue assessment of steel half-pipes bolted connections using local approaches", *Proc. Struct. Integr.*, **1C**, 118-125.
- Paris, P.C. and Erdogan, F. (1963), "A critical analysis of crack propagation laws", *J. Bas. Eng.*, **85**, 528-534.
- Ramberg, W. and Osgood, W.R. (1943), *Description of Stress-Strain Curves by Three Parameters*, NACA Tech. Note No. 902.
- Sanches, R.F., De Jesus, A.M.P., Correia, J.A.F.O., Silva, A.L.L. and Fernandes, A.A. (2015), "A Probabilistic fatigue approach for riveted joints using monte carlo simulation", *J. Constr. Steel Res.*, **110**, 149-162.
- SAS-Swanson Analysis Systems Inc (2008), ANSYS, Houston, Version 11.0.
- Silva, T. (2006), *Trezói Bridge-Study on the Fatigue Behaviour of Riveted Joints in Steel Bridges Ancient*, FEUP/DEMEGI, Project Report on Graduation.